energies

MDPI

Article

Real-Time Analysis of the Impedance–Temperature Relationship in Electric Distribution Lines Using PMUs

Elvia-Andrea Sánchez-Moctezuma [1], Laura-Jaqueline Santander-Hernández [1], Fernanda Álvarez-Mendoza [2] and César Angeles-Camacho [2,*]

[1] Facultad de Ingeniería Eléctrica, Universidad Michoacana de San Nicolas de Hidalgo, 58000 Morelia, Mexico; esanchezmo@ii.unam.mx (E.-A.S.-M.); laura.santander@umich.mx (L.-J.S.-H.)
[2] Instituto de Ingeniería, Universidad Nacional Autónoma de México, 04510 Ciudad de México, Mexico; malvarezm@ii.unam.mx
* Correspondence: cangelesc@ii.unam.mx

Abstract: In this paper, an efficient method to compute the phase impedance of a power distribution line is presented. This paper's main interest is to collect and analyze the impedance–temperature profiles in distribution lines by employing real-time phasor measurement units (PMUs) voltage and current measurements. The monitoring system has been developed for microgrids integrating ocean energies within the scope of the Mexican Ocean Energy Innovation Centre (CEMIE-Océano), contributing to marine energy tools' innovation and development. The development tool can easily be applied to other distribution network components or to monitor microgrids with renewable-energy generation.

Keywords: impedance–temperature relationship; power distribution system; PMUs; renewable energy

Citation: Sánchez-Moctezuma, E.-A.; Santander-Hernández, L.-J.; Álvarez-Mendoza, F.; Angeles-Camacho, C. Real-Time Analysis of the Impedance–Temperature Relationship in Electric Distribution Lines Using PMUs. *Energies* **2021**, *14*, 1661. https://doi.org/10.3390/en14061661

Academic Editor: Adrian Ilinca

Received: 11 February 2021
Accepted: 10 March 2021
Published: 17 March 2021

1. Introduction

In the planning and modeling of networks, the influence of temperature on power system devices is neglected, resulting in imprecise network analyses [1]. The impedance of a conductor changes on the basis of temperature and, in electrical systems, plays one of the most significant roles in analyzing an electrical system; it is an essential indicator for adjusting relays and wide-area monitoring of energy systems [2]. Knowing the impedance values of an overhead line in real time allows us to have a more accurate diagnosis of the network behavior, and, consequently, to make decisions related to the network's load capacity, thermal limit, reliability, and low-performance stress conditions [3,4].

The main limitation in integrating renewable energies into distribution networks (DNs) is the remote locations of most renewable resources [5–7]. Additionally, the connecting network sometimes must be exposed to extreme natural changes, like ocean energies found in high-temperature zones. Conductors are subjected to temperature variations affecting the line's impedance behavior through excessive losses, impairment of the conductor-insulating dielectric, overheating the network, thermal efforts, degradation of the conductor, and others [8].

DN operators face multiple challenges arising from renewable energy, electric cars, batteries, and further electrification; these affect energy quality by varying the demand for load [9–11]. The traditional way to obtain electrical parameters and compute impedance in distribution lines is on the basis of the lines' geometric structures, the conductor's dimensions, approximations of the length of the lines, and the conductors' separation [12,13]. These calculations are only approximations of impedance, ignoring the value of the temperature variation that the conductors are exposed to [14].

Because of these issues, there is growing interest in performing a more detailed analysis of large-scale power systems in DNs. In [15], researchers estimated the parameters of an unbalanced distribution line belonging to a three-phase test network, considering

systematic errors and measurements by PMUs. In [16], researchers focused on model reduction of a DN for state estimation based on PMUs and performed arbitrary selection of lines and network nodes based on load flow equations. In [17], researchers performed detection and localization of changes in the DN topology using data obtained by PMUs. This approach did not require information about the network model or particular characteristics of the disturbance. In addition, other options for monitoring variables in a synchrophasor DN have been reported, such as the micro-PMUs reported in [18]. In DNs, power flow is monitored without prior knowledge of the network topology with the use of phasor measurements as reported in [19]. In [20], two contingencies in the Enduris DN were modeled using real-time power flow values from a PMU and from the control and data acquisition system. This methodology formed the basis for calculating the initial condition of the load flow during each of the network contingencies.

Other researchers have focused on high impedance fault [21–24]. In [24], the impedance calculation was performed through the equivalent of Thevenin for power transfer limits in terms of voltage stability using a PMU. The researchers in [14] explored the admittance matrix of a polyphaser power DN from limited voltage- and current-measurement PMUs. Manageable convex programs were proposed to retrieve the admittance matrix under various scenarios and to track the changes. In [10], researchers presented an algorithm based on weighted least squares (WLS) for the simultaneous estimation of multiple impedances in multiple branches in a single-phase DN, using a monitoring system based on PMUs. In [25], researchers proposed a method to estimate transmission line pi-model impedance parameters and correct the PMUs for the presence of systematic errors in the measurements.

Contrary to previous studies, the objective of this paper is to analyze impedance during temperature changes that disturb the system. An innovative method to compute an overhead line's impedance using phasor measurement units is introduced in this work. As a result, a novel system to monitor the impedance of a low-voltage test network without using the traditional models, but employing PMUs instead, is presented. PMUs provide voltage and current phase and angle and frequency oscillations at different points. These data increase the capabilities of network analysis software and support a more accurate system model. Line parameter estimation studies using PMUs have been reported in the literature [10,15,16]. The analysis of the temperature impact on impedance has also been considered, as reported in [2]. In contrast to these studies, the present paper conducts real-time monitoring of line impedance simultaneously in the presence of temperature variations. This work's contribution is a new approach to computing impedance profiles in real time, taking into consideration the impedance variation related to temperature changes.

2. Methodology

This work used the test network installed in the Power Electronics Laboratory of the Institute of Engineering of the National Autonomous University of Mexico (II-UNAM). The previous work consisted of a low-voltage test network of 220 V, in which a graphical application was developed to monitor the test network in real time using phasor monitoring systems [26,27]. The test network and monitoring system are adapted and updated for the simulation of the network's impedance.

Figure 1 shows the flowchart step by step. This paper's contributions are the real-time impedance calculation shown in the flowchart, the visualization of this information in real time, and its storage for off-line studies.

The application was programmed in LabVIEW to calculate the impedance of the line in real time and the oscillography of voltage and current phasors for each phase, considering Ohm's law in AC. The impedance value is obtained in the form of the relation between voltage and current as follows:

$$Z = \frac{\overline{V}}{\overline{Y}} \tag{1}$$

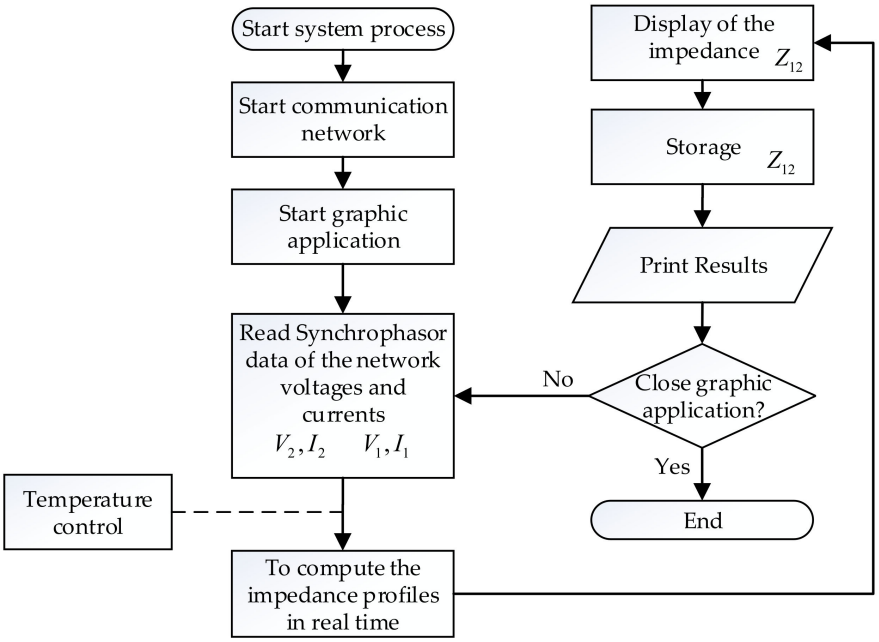

Figure 1. Flowchart of the graphical application.

The calculation of impedance occurs in the form of a phasor. To calculate the impedance value, it was necessary to implement a graphical code to obtain the phases' impedance, as shown in Figure 2 for phase A. This procedure was carried out for each phase of the network.

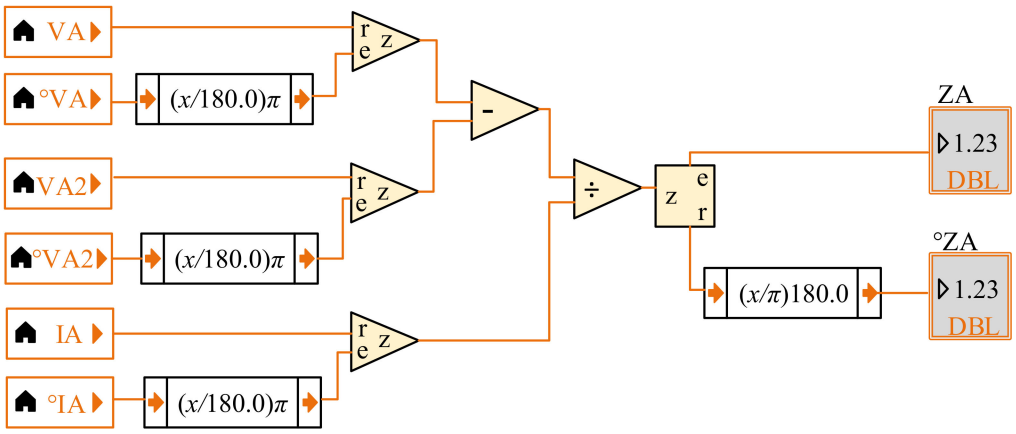

Figure 2. Calculation of the impedance of phase A.

It is important to remark that the validation of the test system's measurements was accomplished through its modeling and simulation in the PSCAD software.

The test network was subjected to various scenarios, consisting of varying a load of its phases at different temperatures and obtaining voltage and current measurements through phasor measurement units. The next step was implementing a system that allows devices to experience temperature changes to apply the climatic variations to which they are exposed in real life. Subsequently, the corresponding tests were carried out at different temperatures to understand the impedance behavior for each phase when the conductor starts to warm up to obtain the relationship between the impedance and the temperature in the distribution lines.

3. Test Network

A wide-area measurement system (WAMS) was implemented for real-time monitoring of a low-voltage test network. For data measurement, the test network had two PMUs, from Schweitzer Engineering Laboratories, Inc. 2350 NE Hopkins Court Pullman, WA USA an SEL-351A at the network input and an SEL-487E at the output, to transmit information to a phasor data concentrator (PDC) named PDC UD-UNAM. Afterward, the data were stored in a database in Microsoft Access and transmitted in a local network under the TCP/IP protocol. The PDC was developed using graphical programming based on LabVIEW, in which a graphical interface was recreated for the user and operator through screens in the workstations. Figure 3 presents the scheme of the implemented test network and the main blocks; it is important to mention that the SEL-2410 is a satellite synchronization clock installed outdoors.

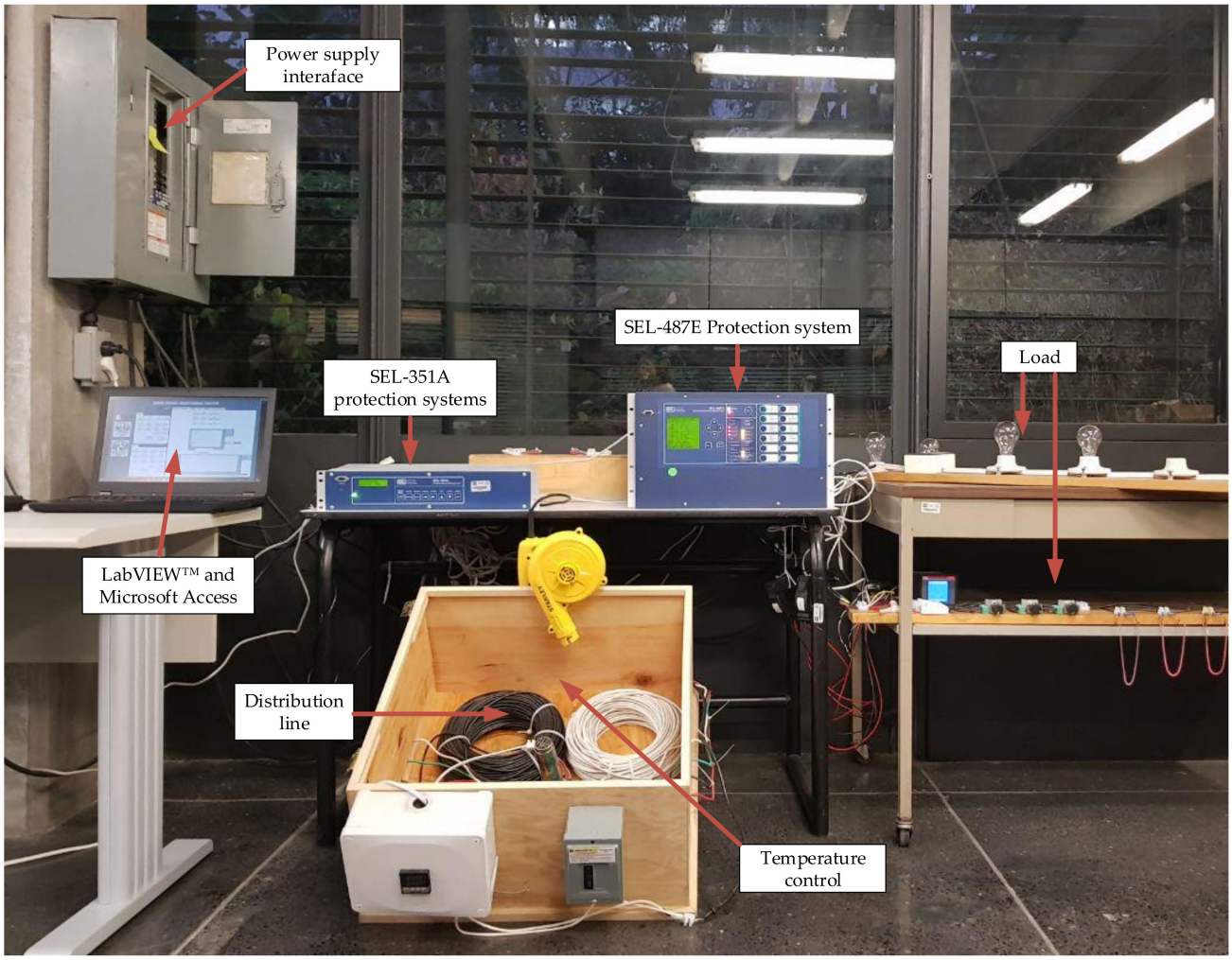

Figure 3. Installation of the test network.

An experiment to demonstrate the electrical effects of a line exposed to temperature variations was designed to have a parameterized model of the electrical lines, which updates the line impedance data in real time to establish a profile of the impedance–temperature relationship of the electrical cables of the test system. The single-line diagram of the modified test network for applying heat to the test network is shown in Figure 4.

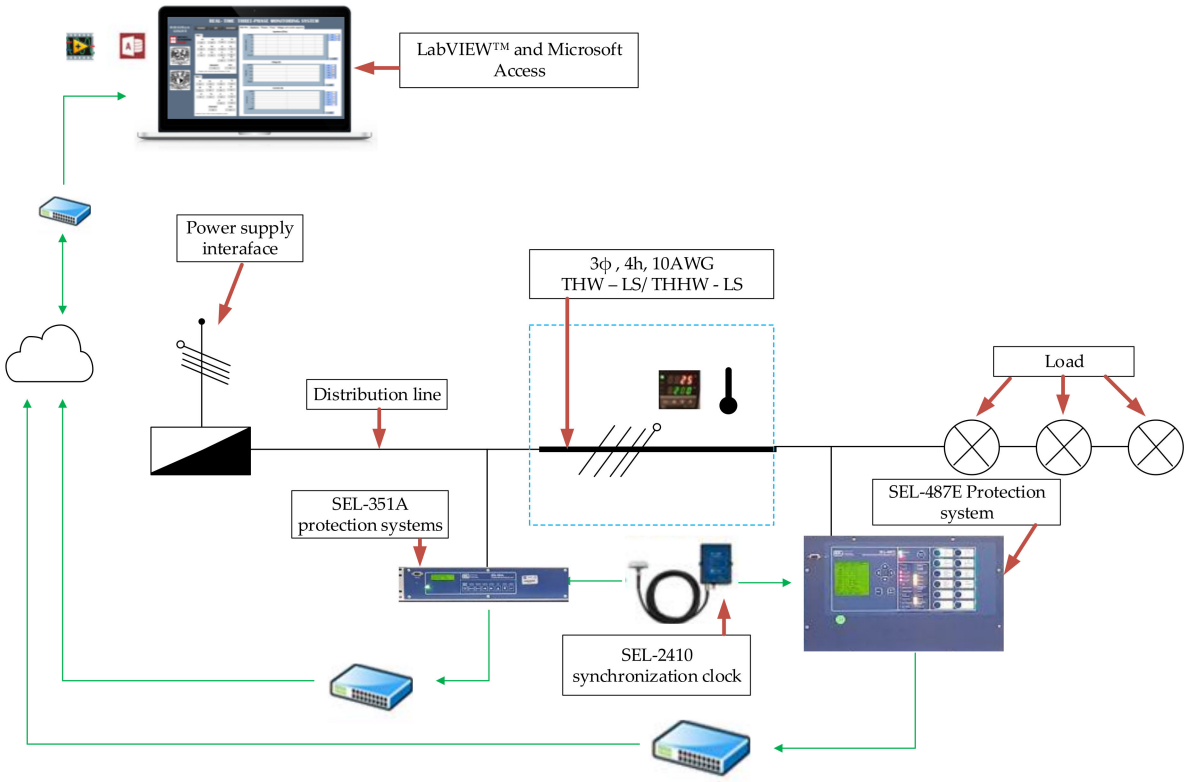

Figure 4. Installation of the test network.

3.1. Temperature Control and Monitoring Process

The conductors were encapsulated in a thermal box to control the heating process, which was controlled with a pyrometer and an air blower. A digital thermometer monitored the temperature. The control process steps applied for temperature variation and measurement were as follows, and the circuit implemented can be seen in Figure 5:

1. The conductors were encapsulated in a thermal box, as shown in Figure 3.
2. The temperature was set to the desired value using a REX C-100 (Tokyo, Japan) pyrometer.
3. The resistance of 10 Ω varied according to the temperature programmed in the pyrometer; thus, the box's interior containing the conductors was heated.
4. The solid-state relay (SSR) worked as a temperature regulator. It is a semiconductor equivalent to the electromechanical relay that can be employed to control electrical loads without moving parts.
5. The temperature sensor was inside the box, next to the conductors, to measure the temperature of the line conductors that were exposed.

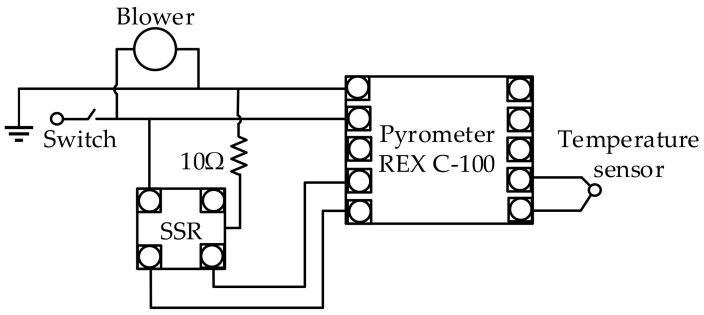

Figure 5. Schematic circuit of the temperature meter.

The main screen of the PDC can be observed in Figure 6, from which the user has access to other tabs, such as instantaneous voltage; instantaneous current; impedance;

frequency; frequency derivative; voltage and current phasors; sequences of voltages and currents; and active, reactive, and apparent power.

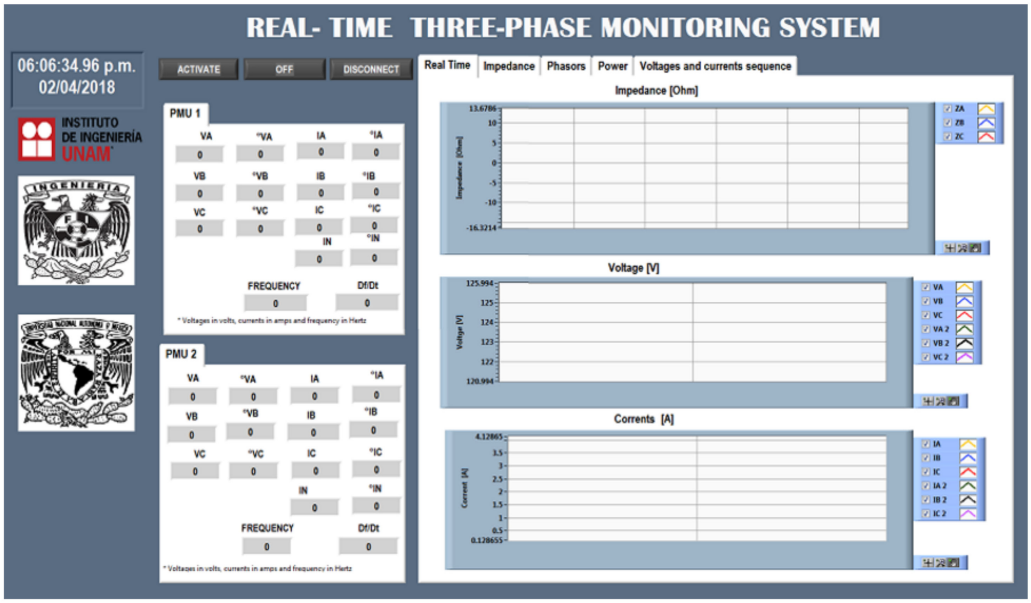

Figure 6. Main screen of the real-time monitoring system.

3.2. Test Network: Modeling and Simulation in Commercial Software

The traditional way of designing and operating a distribution system is through its modeling and simulation in commercial or proprietary software; this allows software designers to establish the system's operating parameters using a mathematical model of lines.

The test network described above and implemented in this study was modeled and simulated in commercial software. The software employed for validation and comparison was PSCAD, where the modeling of a three-phase system, type resistive/inductive (RL), is considered, as described in Figure 7. The value of capacitance was ignored because it is a short line. The measured phase voltages that feed the test network were 125.8, 124.4, and 125.2 V for phases A, B, and C, respectively. The resistors' parameters and the inductances of the test network were measured at each phase of the system, employing a True-RMS Multimeter FLUKE 175 multimeter; the values obtained are presented in Table 1.

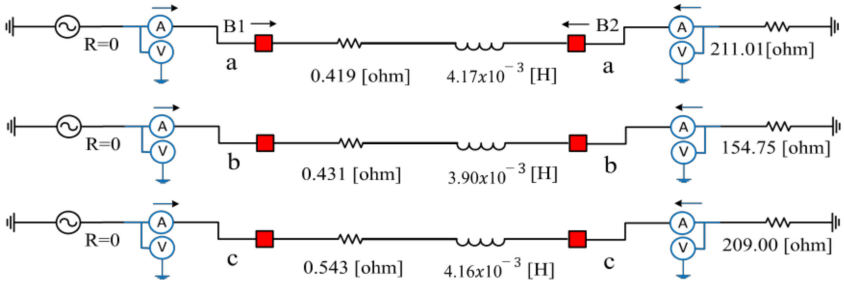

Figure 7. Model of the network.

Table 1. Parameters of the test network.

Phase	Resistance, Ω	Inductance, H	Capacitance, μF
a	0.419	4.173	6.052
b	0.431	3.900	6.476
c	0.543	4.199	6.062

The model was designed with independent power sources for each phase. Each phase of the system line had two multimeters connected in series, allowing us to know the value of instantaneous voltages and currents at the line's input and output. The two switches at the ends of the lines simulated the three-phase logic behavior's operation: 0 = ON for closed and 1 = OFF for open.

To simulate the network in PSCAD, initially, all the values of voltages and currents needed to be increased. Then, thanks to the fast Fourier transform (FFT), we obtained the magnitudes and phases of our input variables, and from them, we computed the sequence components.

$$\begin{bmatrix} V_a \\ V_b \\ V_c \end{bmatrix} = \frac{1}{3} \begin{bmatrix} 1 & 1 & 1 \\ 1 & 1\angle 120^\circ & 1\angle 120^\circ \\ 1 & 1\angle 120^\circ & 1\angle 120^\circ \end{bmatrix} \begin{bmatrix} V_0 \\ V_+ \\ V_- \end{bmatrix} \tag{2}$$

In PSCAD, we can choose the FFT configuration. For our simulation, we used a three-phase system, with a base frequency of 60 Hz, a reference cosine signal, and RMS values in the magnitude of the output signal. Finally, the phase of the wave was given in degrees. The loads connected to the phases were composed of incandescent lamps, were independent of each other, and were modeled in a resistive manner. Given that the power and voltage values are known, the resistance of each lamp was calculated as follows:

$$R = \frac{V^2}{P} \tag{3}$$

Table 2 contains the values of power, voltage, and resistance at each phase.

Table 2. Power, voltage, and resistance values of the installed load in the test network.

Phase	Power, W	Voltage, V	Resistance, Ω
a	72	125.8	219.80
b	72	124.4	214.93
c	72	125.2	217.70

The impedance results obtained from the simulation in PSCAD are visible in Figure 8. It is evident how impedance remains constant at the programmed value during the time of the simulation, regardless of voltage variations or load. The impedances in PSCAD gave us constant values in the three phases, namely $Z_a = 1.6906\ \Omega$, $Z_b = 1.5998\ \Omega$, and $Z_c = 1.7374\ \Omega$.

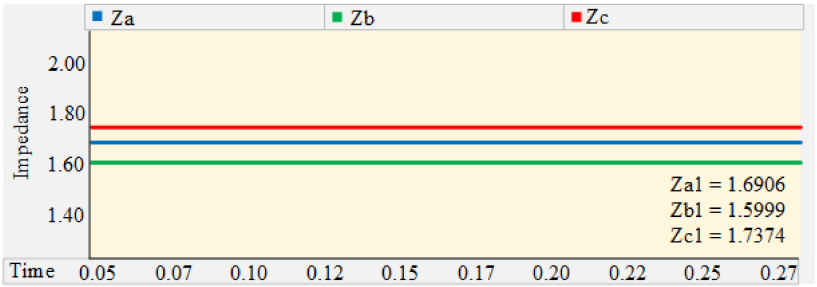

Figure 8. Impedance graph from PSCAD.

4. Cases of Study

The different cases to which the test network was subjected involved modifying the load at each phase of the line and temperature. Several combinations were assessed. However, in the scope of this work, only the following cases are presented:

- Impedance behavior with a balanced load at a constant temperature;

- Impedance behavior with a balanced load at two different temperatures;
- Impedance behavior with a balanced load at a gradually increasing temperature;
- Impedance behavior with an unbalanced load at a gradually increasing temperature.

The test system allowed the visualization of the voltage and current synchrophasor in the measurement points and all the parameters specified in the screens above. However, only the corresponding tabs focused on obtaining the line's phase impedance values. The measurements of voltage and current in sequence were presented in real time.

The impedance values obtained in the line phases, in each case presented, were validated through modeling and simulation of the test system in the PSCAD software. The analysis results allowed us to validate our test system in LabVIEW and establish the differences between a mathematical model and a parameterized model when studying a power line.

4.1. Impedance Behavior with a Balanced Load at a Constant Temperature

In this case, the aim was to detect an overhead line's actual behavior profile at room temperature. The load installed in the phases was balanced and compounded by incandescent bulbs of 72 W; the test was carried out at a constant temperature of 25 °C for 15 min. The results obtained from the test in the network are shown in the developed PDC system's secondary windows presented in Figure 9, where the balanced charges can be observed.

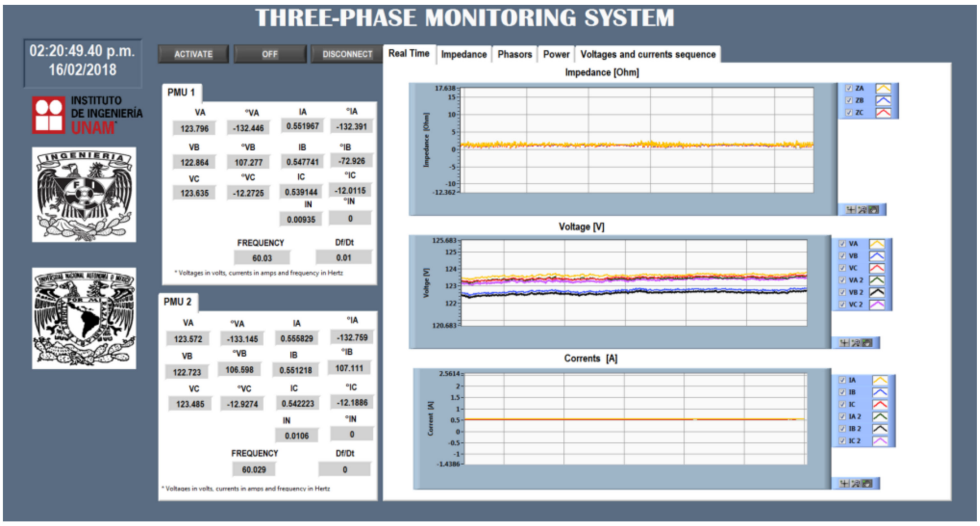

Figure 9. Real-time screen of phasor data concentrator (PDC) UD-UNAM.

The impedances of the conductors are very alike, with oscillations between 0.39 and 2.53 Ω. The currents in the phases overlapped with each other because the connected load was balanced. In contrast, the phase voltages measured from the test network differed when compared between them; this is more noticeable in phase b at the sending and receiving nodes, which is a consequence of the imbalance given in the network's power supply.

To compare the results of a parametric model, such as the ones gathered using the developed PDC system, and a typical mathematical model used in commercial software, both results have been plotted in Figure 10, where the impedance fluctuation can be noted. Furthermore, Table 3 shows the maximum and minimum impedances retrieved by the PDC.

Table 3. Impedance values of the PDC.

	Minimum, Ω	**Maximum, Ω**
Z_a	0.3954	2.539
Z_b	0.2888	2.525
Z_c	0.2523	2.404

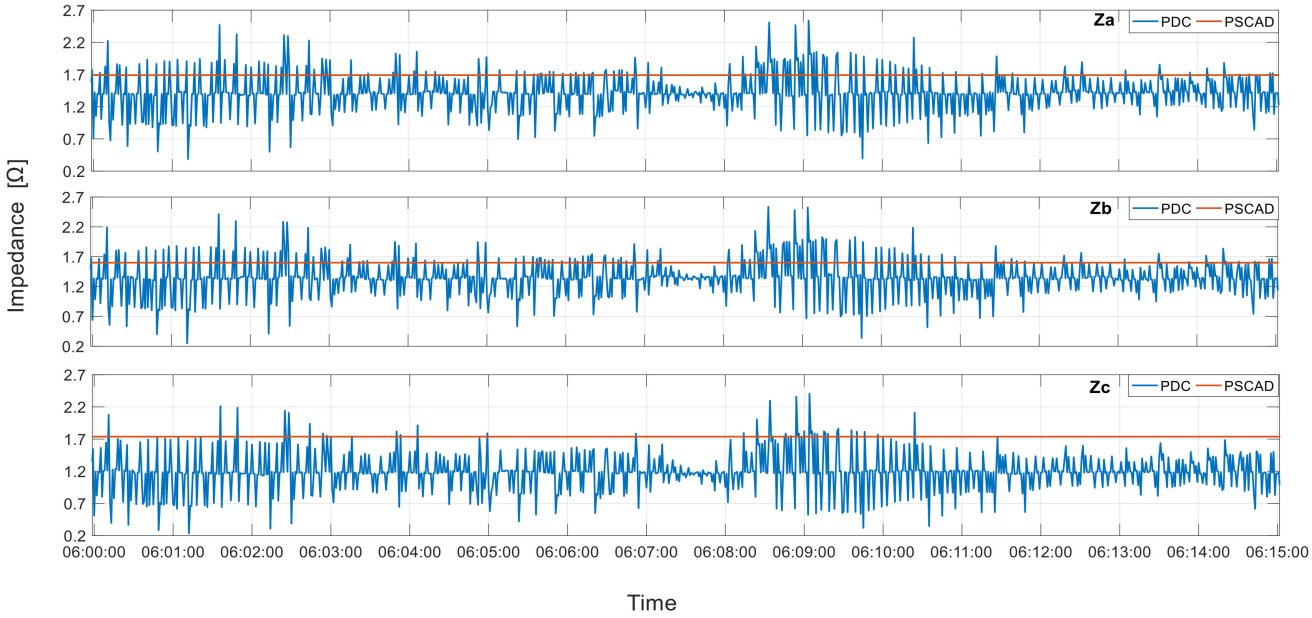

Figure 10. Comparison of PSCAD vs. PDC for impedance in phase a, b and c.

4.2. Impedance Behavior with a Balanced Load at Two Different Temperatures

In this case, the test network was subjected to two different constant temperatures of 25 and 45 °C, with a balanced load of 72 W; the devices were kept at the aforementioned temperatures for 10 min in both cases to compare the two impedance profiles.

As shown in Figure 11, the increase in impedance was evident as the temperature grew; a significant distortion in the impedance was detected when the cables were exposed to an increase in temperature.

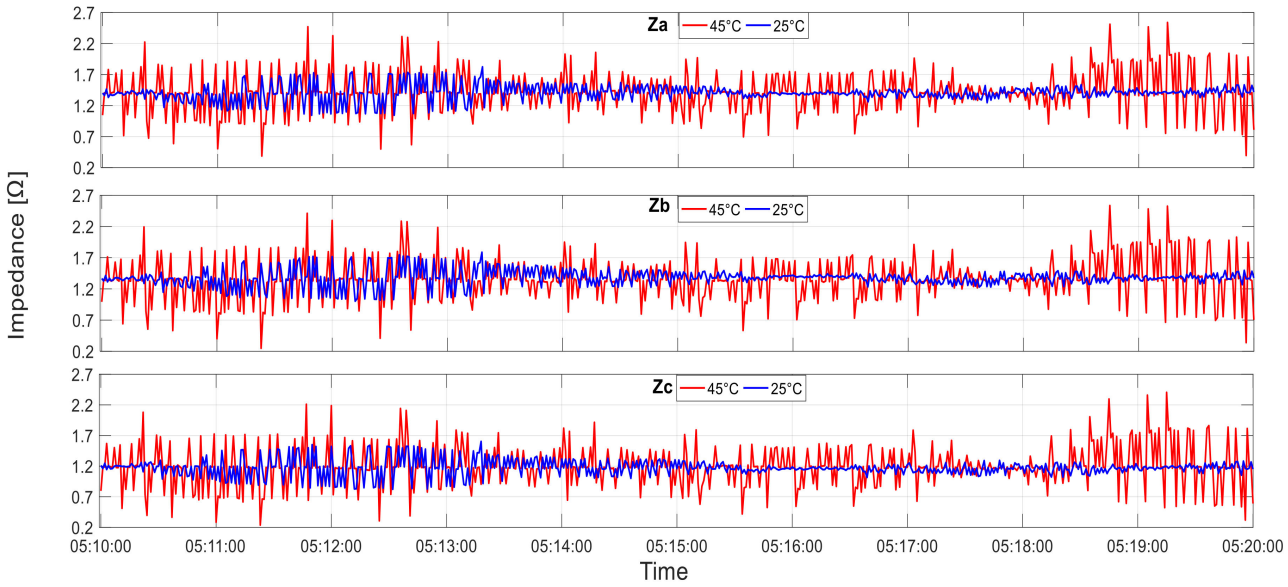

Figure 11. Impedance in phase a, b and c profiles for temperatures 25 and 45 °C.

4.3. Impedance Behavior with a Balanced Load at a Gradually Increasing Temperature

In this case, the load installed at each phase was balanced by incandescent bulbs of 72 W. The test consisted of increasing the temperature from 25 to 52 °C, emulating the temperature changes of tropical zones and reaching an extreme temperature. The temperature increments were made in 3 °C steps, with a ±2 °C variation between each of

the measurements taken in 10 min intervals. The collected impedance profile is seen in Figure 12.

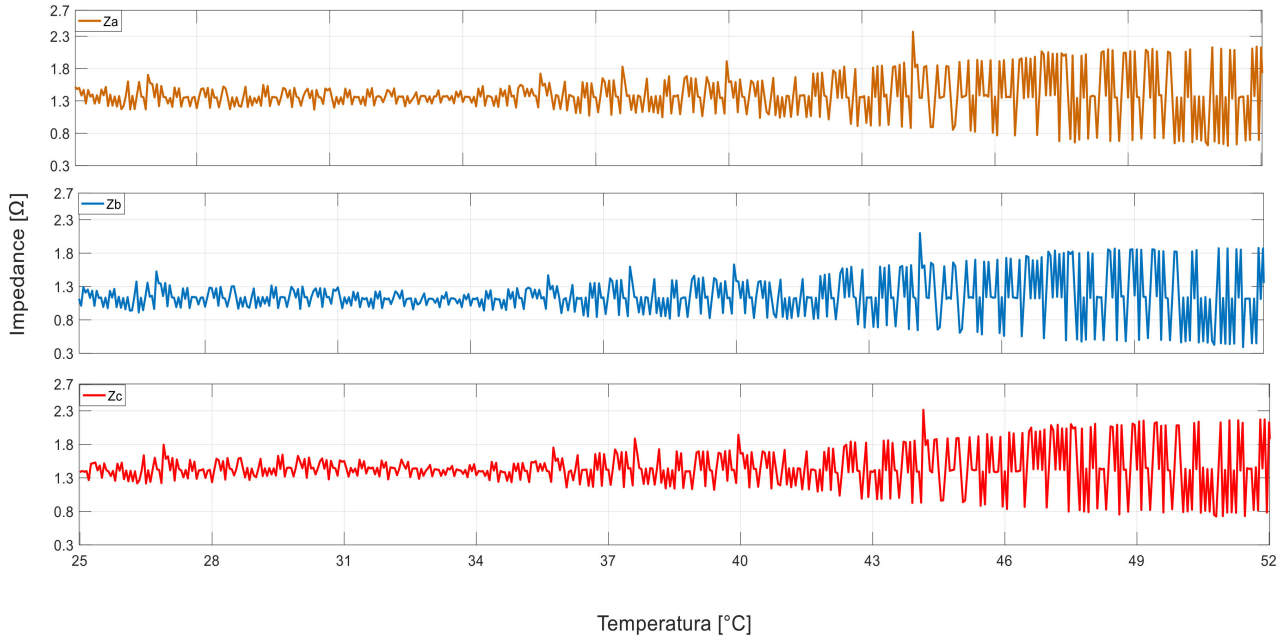

Figure 12. Impedance in phase a, b and c profiles when increasing the temperature from 25 to 52 °C.

The impedance in phases a and c presented practically the same behaviors, with a maximum impedance value of 2.49 Ω, whereas phase b presented a maximum impedance value of 2.37 Ω. As mentioned above, in this case, the loads were balanced to expect similar behavior in the impedance of the line's phases, but the imbalance of the phases' power supply was visible in phase b.

4.4. Impedance Behavior with an Unbalanced Load at a Gradually Increasing Temperature

To obtain a temperature impedance profile from a line closer to reality, a case study was conducted with an unbalanced system. The charges were as follows: Phase a: an incandescent bulb of 72 W and 110 W; Phase b: a 100 W incandescent bulb; Phase c: a 75 W incandescent bulb. Figure 13 shows the impedance–temperature profile obtained.

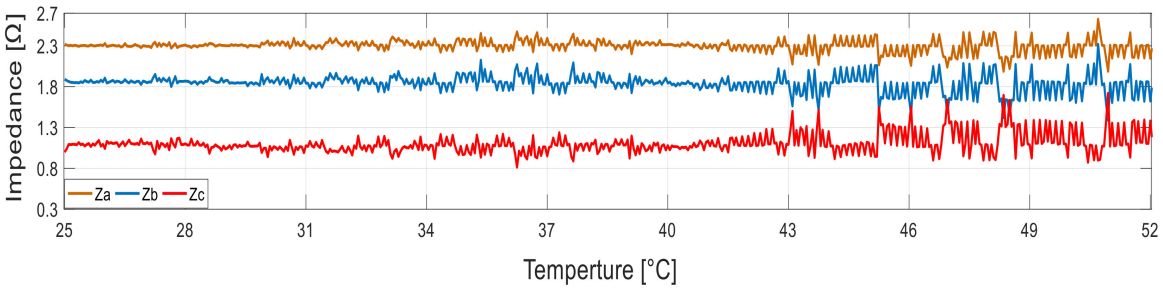

Figure 13. Impedance profiles when increasing the temperature from 25 to 52 °C in an unbalanced system.

The results in Figure 13 demonstrate the apparent distortion and increase in the impedance of the cables when subjected to a rise in temperature; the impedance in each phase had different behavior from that of each other phase, a consequence of the imbalance of the loads.

5. Discussion

In all results obtained from the proposed system, the fluctuating behavior of the impedance is very noticeable, and temperature plays a vital role in it.

The difference between the mathematical models used in commercial software and the parametric line model in almost real time proposed in this article lies in the fact that the parametric line models are real approximations in the proposed approach. These model approximations are based on actual data obtained from the system, including its specific temperature exposition, giving the flexibility to be adapted to any network, as seen in Figures 8 and 10.

From the first case, it is remarkable how the PSCAD simulation indicates that the impedance values are constant on the basis of its mathematical model, unlike the PDC which shows the variation of the impedance in real time, as expected; it is observed that the three lines have similar behavior when the load is balanced.

Analyzing Figure 11 and comparing the line impedance at 25 and 45 °C, it is noticeable that the impedance–temperature relationship is not linear, which gives more importance to this study. Comparing this result with the ones shown in Figure 12 shows how the impedance distortion and the cable impedance value grow as temperature increases. Furthermore, the impedance–temperature relationship in unbalanced networks allows managing overhead lines' capability in a more precise manner.

6. Conclusions

Nowadays, the electricity industry has adopted renewable resources as new sources of energy by incorporating new systems. The proposed system in this paper proved to be a useful tool for monitoring line impedance in real time.

Obtaining parameters that affect impedance in real time will require parametric models of the lines used in conventional studies, including power flow and state estimation. In this sense, we conclude that this computational tool is an efficient way to monitor phase impedance, which could help us to achieve the following objectives:

- Understanding the lines' behavior;
- Knowing the type of compensation required for proper functioning of the line;
- Planning more accurate studies that include renewable generation;
- Controlling load levels;
- Obtaining a parametric model of the line.

It is important to note that the analysis of the impedance–temperature relationship demonstrates that the temperature negatively influences the impedance. Replicating a system of this type can be used to establish impedance–temperature profiles for critical lines in networks or to adjust distribution models and transmission lines and thus predict their behavior when the conductors are subjected to different temperature levels. Such a system can also be used to extend the life of the devices, which is affected by variations in impedance.

With the values obtained from the proposed system, the following types of studies can be carried out:

- Off-line;
- On-line;
- Postmortem.

This type of visualization tool can improve the diagnostic and updating capabilities of network analysis software and support models that are more precise in general distribution networks, allowing better model validation, detection and location of events, and characterization of resources and renewable charges, among other applications.

With this type of study, we can create portfolios of impedance–temperature profiles that allow us to conduct studies on electrical lines using accurate simulations for planning and line design.

The impedance–temperature relationship can be integrated into simulations concerning distribution networks. The results obtained would be approximate to reality when the overhead lines are exposed to temperature changes, something that simulation programs neglect in their analysis.

Finally, but no less important to mention, is that the developed tool can be used in real-time analysis, such as hosting capacity, parameter identification, situational awareness, state estimation, and the modeling of elements in electrical networks.

Author Contributions: Conceptualization, writing—original draft, writing—review and editing, software, investigation, and visualization: E.-A.S.-M.; writing—review and editing and resources: L.-J.S.-H.; writing—review and editing, data curation, software, and investigation: F.Á.-M.; and writing—review and editing, validation, and providing the final approval of the version to publish: C.A.-C. All authors have read and agreed to the published version of the manuscript.

Funding: The authors are grateful to the Centro Mexicano de Innovación en Energía del Océano (CEMIE-Océano) funded by CONACYT-SENER Sustentabilidad Energetica, project: FSE-2014-06-249795 for its financial and technical support. his research was funded by the National Council of Science and Technology of Mexico (CONACYT), through grant number 592994.

Institutional Review Board Statement: Not applicable.

Informed Consent Statement: Not applicable.

Acknowledgments: The authors would like to thank the reviewers for their constructive comments, which have improved the quality of this paper.

Conflicts of Interest: The authors declare no conflict of interest.

References

1. Kersting, W.H. *Distribution System Modeling and Analysis*; Taylor & Francis: Boca Raton, FL, USA; CRC Press: Boca Raton, FL, USA, 2017.
2. Zainuddin, N.M.; Rahman, M.S.A.; Kadir, M.Z.A.A.; Ali, N.H.N.; Ali, Z.; Osman, M.; Mansor, M.; Ariffin, A.M.; Nor, S.F.M.; Nasir, N.A.F.M.; et al. Review of Thermal Stress and Condition Monitoring Technologies for Overhead Transmission Lines: Issues and Challenges. *IEEE Access* **2020**, *8*, 120053–120081. [CrossRef]
3. Rakpenthai, C.; Uatrongjit, S. Power System State and Transmission Line Conductor Temperature Estimation. *IEEE Trans. Power Syst.* **2017**, *32*, 1818–1827. [CrossRef]
4. Sanchez-Moctezuma, E.A. Development of a Computational Tool for the Study of the Impedance-Temperature Relationship in Distribution Lines, Using PMUs. Bachelor's Thesis, National Autonomous University of Mexico, Mexico City, Mexico, March 2018.
5. Telukunta, V.; Pradhan, J.; Agrawal, A.; Singh, M.; Srivani, S.G. Protection challenges under bulk penetration of renewable energy resources in power systems: A review. *CSEE J. Power Energy Syst.* **2017**, *3*, 365–379. [CrossRef]
6. Venkateswaran, V.B.; Saini, D.K.; Sharma, M. Approaches for optimal planning of energy storage units in distribution network and their impacts on system resiliency. *CSEE J. Power Energy Syst.* **2020**, *6*, 816–833. [CrossRef]
7. Tian, X.; Zhang, J.; Li, X.; Zhao, L.; Wu, J. Analytics of high-penetration renewable energy accommodation using power system operation simulation. *J. Eng.* **2018**, *17*, 1889–1895. [CrossRef]
8. Buhari, M.; Levi, V.; Awadallah, S.K.E. Modelling of Ageing Distribution Cable for Replacement Planning. *IEEE Trans. Power Syst.* **2016**, *31*, 3996–4004. [CrossRef]
9. Stecca, M.; Elizondo, L.R.; Soeiro, T.B.; Bauer, P.; Palensky, P. A Comprehensive Review of the Integration of Battery Energy Storage Systems Into Distribution Networks. *IEEE Open J. Ind. Electron. Soc.* **2020**, *1*, 46–65. [CrossRef]
10. Pegoraro, P.A.; Brady, K.; Castello, P.; Muscas, C.; Von Meier, A. Line Impedance Estimation Based on Synchrophasor Measurements for Power Distribution Systems. *IEEE Trans. Instrum. Meas.* **2019**, *68*, 1002–1013. [CrossRef]
11. Jia, L.; Tong, L. Renewables and Storage in Distribution Systems: Centralized vs. Decentralized Integration. *IEEE J. Sel. Areas Commun.* **2016**, *34*, 665–674. [CrossRef]
12. Grainger, J.J.; Lozano Sousa, C. *Análisis de Sistemas de Potencia*, 2nd ed.; Mc. Graw Hill: Mexico City, Mexico, 1997.
13. Acha, E.; Fuerte-Esquivel, C.R.; Ambriz-Perez, H.; Angeles-Camacho, C. *FACTS: Modelling and Simulation in Power Networks*, 1st ed.; John Wiley & Sons: Hoboken, NJ, USA, 2004; p. 420. ISBN 978-0-470-02015-9.
14. Ardakanian, O.; Wong, V.W.; Dobbe, R.; Low, S.H.; von Meier, A.; Tomlin, C.J.; Yuan, Y. On Identification of Distribution Grids. *IEEE Trans. Control Netw. Syst.* **2019**, *6*, 950–960. [CrossRef]
15. Puddu, R.; Brady, K.; Muscas, C.; Pegoraro, P.A.; Von Meier, A. PMU-Based Technique for the Estimation of Line Parameters in Three-Phase Electric Distribution Grids. In Proceedings of the IEEE 9th International Workshop on Applied Measurements for Power Systems (AMPS), Bologna, Italy, 26–28 September 2018; pp. 1–5. [CrossRef]

16. Carta, D.; Benigni, A.; Muscas, C. Model Order Reduction for PMU-Based State Estimation in Distribution Grids. *IEEE Syst. J.* **2018**, *12*, 2711–2720. [CrossRef]
17. Mayo-Maldonado, J.C.; Valdez-Resendiz, J.E.; Guillen, D.; Bariya, M.; Von Meier, A.; Salas-Esquivel, E.A.; Ostfeld, A. Data-Driven Framework to Model Identification, Event Detection, and Topology Change Location Using D-PMUs. *IEEE Trans. Instrum. Meas.* **2020**, *69*, 6921–6933. [CrossRef]
18. Farajollahi, M.; Shahsavari, A.; Stewart, E.M.; Mohsenian-Rad, H. Locating the Source of Events in Power Distribution Systems Using Micro-PMU Data. *IEEE Trans. Power Syst.* **2018**, *33*, 6343–6354. [CrossRef]
19. Sankur, M.D.; Dobbe, R.; Von Meier, A.; Arnold, D.B. Model-Free Optimal Voltage Phasor Regulation in Unbalanced Distribution Systems. *IEEE Trans. Smart Grid.* **2020**, *11*, 884–894. [CrossRef]
20. Save, N.; Popov, M.; Jongepier, A.; Rietveld, G. PMU-based power system analysis of a medium-voltage distribution grid. *CIRED-Open Access Proc. J.* **2017**, *1*, 1927–1930. [CrossRef]
21. Zanjani, M.G.M.; Mazlumi, K.; Kamwa, I. Application of μPMUs for adaptive protection of overcurrent relays in microgrids. *IET Gener. Transm. Distrib.* **2018**, *12*, 4061–4068. [CrossRef]
22. Cui, Q.; Weng, Y. Enhance High Impedance Fault Detection and Location Accuracy via μ-PMUs. *IEEE Trans. Smart Grid.* **2020**, *11*, 797–809. [CrossRef]
23. Sharma, N.K.; Samantaray, S.R. PMU Assisted Integrated Impedance Angle-Based Microgrid Protection Scheme. *IEEE Trans. Power Deliv.* **2020**, *35*, 183–193. [CrossRef]
24. Li, W.; Wang, Y.; Chen, T. Investigation on the Thevenin equivalent parameters for online estimation of maximum power transfer limits. *IET Gener. Trans. Distrib.* **2010**, *4*, 1180–1187. [CrossRef]
25. Ritzmann, D.; Wright, P.S.; Holderbaum, W.; Potter, B. A Method for Accurate Transmission Line Impedance Parameter Estimation. *IEEE Trans. Instrum. Meas.* **2016**, *65*, 2204–2213. [CrossRef]
26. Rocha-Doria, J.S.; Mosquera-Arevalo, O.A.; Angeles-Camacho, C.; Espinel-Ortega, A.; Calderón-Guizar, J.G. Design and implementation of a real-time monitoring tool for power engineering education. *Comput. Appl. Eng. Educ.* **2018**, *26*, 37–48. [CrossRef]
27. Deras-Campos, J.G.; Angeles-Camacho, C.; Cardenas-Guzman, L.; Gomez-Lugo, E.; Valles-Canales, J. A Review of the New Medium Voltage Smart Grid at UNAM and its Academic Uses. In Proceedings of the IEEE PES Innovative Smart Grid Technologies Conference Europe (ISGT-Europe), Sarajevo, Bosnia and Herzegovina, 21–25 October 2018; pp. 1–5. [CrossRef]